

Plasma diagnostics using K-line emission profiles of silicon

YILING CHEN

Universität Rostock



Outline

Motivation

- + K_{α} plasma diagnostics
- + Si K_{α} fluorescence spectra

Theory

- + Line shift due to excitation and ionization
- + Line shift due to plasma environment
- + Plasma composition

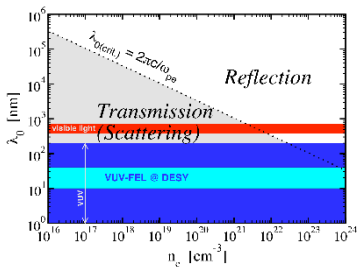
Results

- + Synthetic spectra

Summary and Outlook

K_α plasma diagnostics

- + mid-z materials K_α : in X ray range (100 eV-1 MeV) relevant for diagnostics
- + warm dense matter ($n_e: 10^{20} - 10^{24} \text{ cm}^{-3}$)
- + propagation in warm dense matter
- + modification of spectral line profiles.

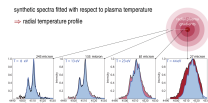
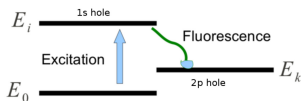
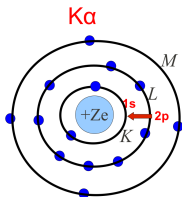


- + $\lambda = \frac{2\pi c}{\omega_{pl}}, \quad \omega_{pl}^2 = \frac{n_e e^2}{\epsilon_0 m_e}$
- + reflectivity $R = \left| \frac{\sqrt{\epsilon}-1}{\sqrt{\epsilon}+1} \right|^2$
- + long wavelength limit $k \rightarrow 0$
- + $\lim_{k \rightarrow 0} \epsilon^{RPA} = 1 - \frac{\omega_{pl}^2}{\omega^2}$
- + $\omega_{pl} < \omega, R < 1$
- + $\omega_{pl} > \omega, R = 1$

K_{α} emission line in fluorescence spectra

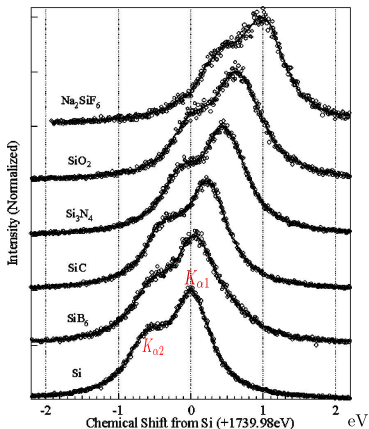
Warm dense matter

- + the electron excitation from E_0 (ground state) to E_i (initial state) and photon emission from E_i to E_k (final state) in K_{α} fluorescence



- + titanium U. Zastrau, A. Sengebusch et al., *High Energy Density Phys.* 7,47-53 (2011)
- + Si: solid density $n_{\text{tot}} = 5 \times 10^{22} \text{ cm}^{-3}$
- + different emitter configurations are considered

Si K_{α} emission line in fluorescence spectra



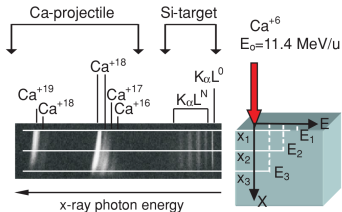
- + K_{α} x-ray fluorescence spectra of pure Si and Si compounds
- + cold emitters $T \approx 1$ eV
- + fine structure $K_{\alpha 1}$ and $K_{\alpha 2}$
- + shifts due to chemical binding depending on chemical surrounding

Zhenlin Liu, Shouichi Sugata, et al., *Phys. Rev. B* **69**, 035106 (2004)

Si emission lines from SiO₂ aerogel

(At UNILAC accelerator at GSI-Damstadt)

+ X-ray emission spectra of low-density SiO₂ aerogel induced by Ca projectiles



+ different penetration depths x
 + different penetration energies E

(a) $x_1 = 0.5 \text{ mm}$ ($E_1 = 11.4 - 10.6 \text{ MeV/u}$)

(b) $x_2 = 5 \text{ mm}$ ($E_2 = 8.5 - 7.6 \text{ MeV/u}$)

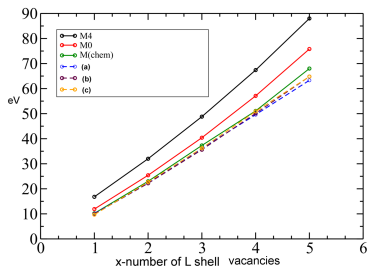
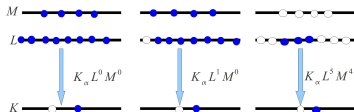
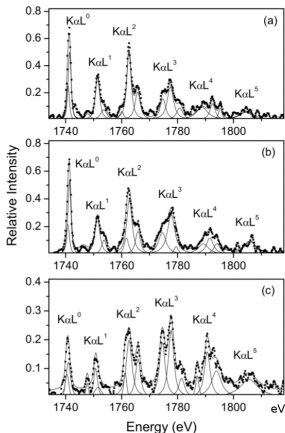
(c) $x_3 = 10 \text{ mm}$ ($E_3 = 5.2 - 4.0 \text{ MeV/u}$)

J. Rzakiewicz, A. Gojska et al., *Phys. Rev. A* **82**, 012703 (2010)

Si $K_\alpha L^x M^y$ satellites,

($x=N=0-5, y=0,4$)

Phys. Rev. A **82**, 012703 (2010)



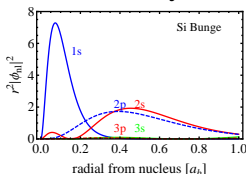
Theory- Blue shift due to excitation and ionization

- + description of isolated ionic emitter H^0 by self-consistent

Roothaan – Hartree – Fock equations. C. C. J.Roothaan (1951).

- + Bunge wave function $\phi_{nlm}(r, \theta, \phi) = R_{nl}(r) \cdot Y_{lm}(\theta, \phi)$

$$R_{nl} = \sum_j S_{jl} C_{jln}$$

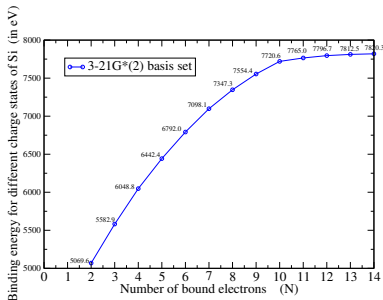


- + Gaussian wave function H. B. Schlegel and M. J. Frisch, *International Journal of Quantum Chem.* 54, 83-87 (1995).

$$G_{\vec{g}}(\vec{r}, l_x, l_y, l_z, \alpha) = N(l_x, l_y, l_z, \alpha) x^{l_x} y^{l_y} z^{l_z} e^{-\alpha \vec{r}^2}$$

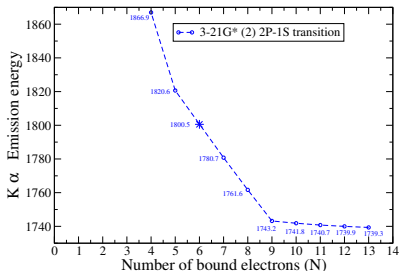
- + unperturbed ionization and emission energies obtained from chemical *ab initio* code G03
- + using Gaussian basis set: 3 – 21G*, 19 basis functions

Binding energy



+ Ground state of Si:
 $1s^2 2s^2 2p^6 3s^2 3p^2$

K_{α} emission energy



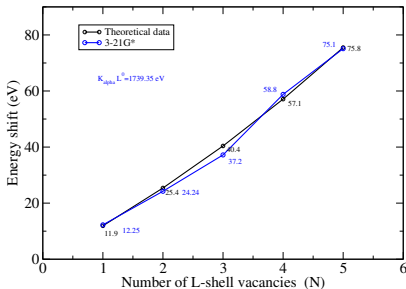
+ for emission of Si^+ (N=13):
 initial state: $1s^1 2s^2 2p^6 3s^2 3p^2$
 final state: $1s^2 2s^2 2p^5 3s^2 3p^2$

$K_\alpha L^N M^0$ and $K_\alpha L^N M^4$

Comparison of the $K_\alpha L^0$ with satellites energy shifts

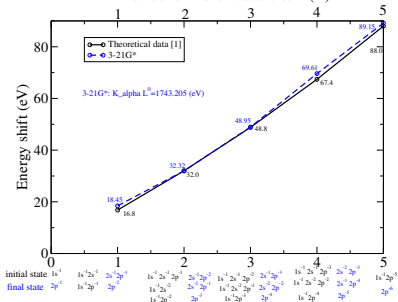
$K_\alpha L^N M^0$

M0: represents the ground-state $3s^2 3p^2$



$K_\alpha L^N M^4$

Number of L-shell vacancies (N)



Theoretical data: J. Rzakiewicz, A. Gojska et al., *Phys. Rev. A* **82**, 012703 (2010)



Red shift due to plasma polarization

- + Ion sphere potential obtained from Poisson-equation :

$$\Delta\phi(r) = 4\pi e n_f(r) + 4\pi e n_b(r) - 4\pi Ze \delta(r)$$

- + density of bound electrons: $n_b = \frac{1}{4\pi} \sum_{nl} |R_{nl}(r)|^2$

- + self-consistency with respect to free electron density:

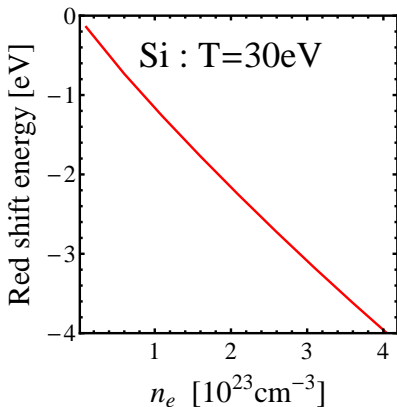
$$n_f(r) \propto \int_{p_0}^{\infty} \frac{dp p^2}{(2mk_B T)^{3/2}} \exp\left[\left(\frac{-p^2}{2mk_B T} + \frac{e\phi(r)}{k_B T}\right)\right], p_0 = \sqrt{2me\phi(r)}$$

- + perturbative ansatz $H = H^0 + H'$ with $H' = -e[\phi(r) - \phi(r, n_f = 0)]$

- + due to plasma shift energies polarization due to plasma screening:

$$\Delta E^{(1)} = \langle \psi_i | H' | \psi_i \rangle - \langle \psi_f | H' | \psi_f \rangle$$

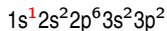
Red shift due to plasma polarization



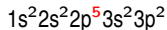
+ using Bunge RHF function

+ configuration of Si^+ :

initial state :



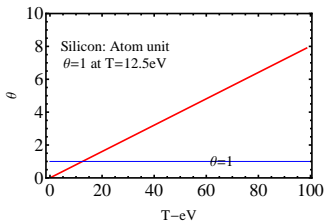
final state :



Plasma Composition

Coupled saha equation

- + Degeneracy parameter $\Theta = \frac{k_B T}{E_{\text{Fermi}}} > 1$, $E_{\text{Fermi}} = \frac{\hbar^2}{2m_e} (3\pi^2 n_e)^{2/3}$
- + Boltzmann distribution function $f_e(p) = e^{-\beta(p^2/2m_e - \mu_e)}$
- + due to relations $\mu_m = \mu_{m+1} + \mu_e$ assuming local thermal equilibrium conditions
- + iteration to be solved : $n_{(m)} = \left[e^{-\mu_e/k_B T} \right]^m \frac{\sigma_{(m)}^{in}}{\sigma_{(0)}^{in}} n_{(0)}$



electron-ion interaction

- + Wigner-Seitz radius R defined by $R = \left(\frac{Z_{ion}}{4\pi n_e} \right)^{1/3}$
- + the ion sphere has Wigner-Seitz radius R to build ion-electron shift :

$$\Delta_e^{ei} = -\frac{Z_{ion}e^2}{4\pi\epsilon_0 R} = -\frac{e^2}{\epsilon_0} \left(\frac{Z_{ion}}{4\pi} \right)^{2/3} \left(\frac{n_e}{3} \right)^{1/3}$$

- + internal partition function of ion-electron shift:
(m : number of ionisation steps)

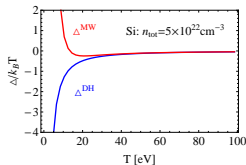
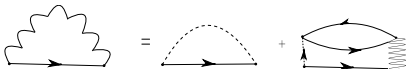
$$\sigma_e^{in}(m) = 2^m \exp \left[\frac{1}{k_b T} \frac{e^2}{(4\pi)^{2/3} \epsilon_0} \left(\frac{n_e}{3} \right)^{1/3} \sum_{x=1}^m x^{2/3} \right]$$

electron-electron interaction

- + then the electronic chemical potential in the classical low density case reads

$$\mu_e = \frac{n_e \lambda_e^3}{2} - \frac{e^2}{2} \sqrt{\frac{n_e e^2}{\epsilon_0 k_B T}} + \frac{\sqrt{2\pi^2} n_e \lambda_e e^4}{8(k_B T)^2} - \frac{n_e \lambda_e^3}{8\sqrt{2}} + \frac{n_e \lambda_e^2 e^2}{4k_B T}$$

- + Montroll-Ward approximation: $= \Delta^{HF} + \Delta^{MW}$



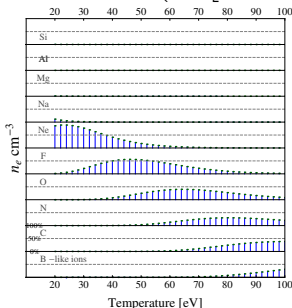
Plasma Composition

Planck-Larkin partition function

$$+ \sigma_e^{in}(m) = 2^m \exp \left[-\frac{\Delta_e^{MW}}{k_B T} \right]^m \exp \left[\frac{1}{k_B T} \frac{e^2}{(4\pi)^{2/3} \epsilon_0} \left(\frac{n_e}{3} \right)^{1/3} \sum_{x=1}^m x^{2/3} \right]$$

+ Planck-Larkin partition function for bound contributions

$$\sigma_e^{in,PL} = \sum_{nl} n_{nl} (2l + 1) \left(\exp \left[-\frac{E_{nl}}{k_B T} - 1 \right] + \frac{E_{nl}}{k_B T} \right)$$





Synthetic spectra

- + average emission power from N_i atoms in state E_i

$$\langle P \rangle_{ik} = N_i \cdot A_{ik} \cdot \hbar \cdot \omega_{ik}$$

- + with spontaneous transition probability,

$$A_{ik} = \frac{2e^2 \omega_{ik}^3}{3\epsilon_0 c^3 \hbar} \left| \frac{1}{\Omega_0} \int \psi_i^* \vec{r} \psi_k d^3 r \right|^2$$

- + with approximation

$$\langle P \rangle_{ik} = N_i E_0 A$$

- + intensity give as

$$\frac{I_{max}}{I_{ref}} = \frac{N_i E_0 A}{N_{ref} E_0^{ref} A_{ref}} \simeq \frac{n}{n_{ref}} \left(\frac{E_0}{E_0^{ref}} \right)^4$$

Synthetic spectra

- + Lorentz profil for individual spectral lines

$$I_{\text{Lorentz}}(E) = \frac{I_{\text{max}}(\gamma/2)^2}{(E - E_0)^2 + (\gamma/2)^2}$$

- + convoluted with Gaussian instrument function

$$I(E) = \int_{-\infty}^{\infty} dz I_{\text{Lorentz}}(E + z) \frac{1}{\sqrt{2\pi}\Gamma_G} \exp\left[-\frac{z^2}{2\Gamma_G^2}\right]$$

- + fixed parameters for Si:

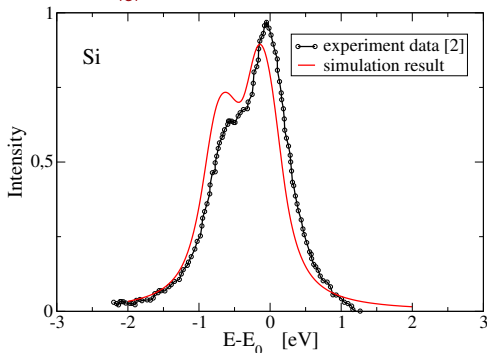
Lorentzian linewidth $\gamma = 0.43$ eV

Gaussian width $\Gamma_G = 0.13$ eV

G.Graeffe, H. Juslen et al., *J.Phys. B: Atom. Molec. Phys.*, Vol. 10, No. 16, 1977

$K_{\alpha} L^0 M^0$ line for Si

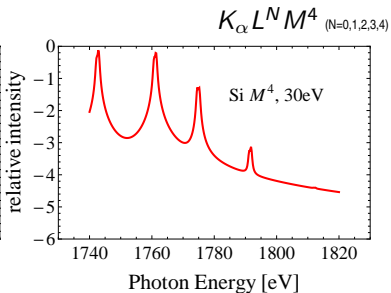
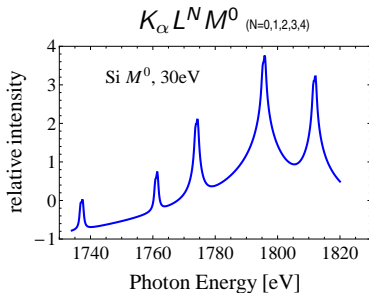
$T = 30$ eV, $n_{\text{tot}} = 5 \times 10^{22} \text{cm}^{-3}$



- + fine structure $P_{3/2}$ and $P_{1/2}$ influence the intensity
- + distance of 0.591 eV between fine-structure components (semi-empirical NIST data)
- + experiment data [2]: Zhenlin Liu, Shouichi Sugata, et al., *Phys. Rev. B* **69**, 035106 (2004)

spectrum with satellite emission lines

temperature = 30 eV



Summary and Outlook

- + X-ray emissions strongly depend on the ion configuration and emitter environment
- + red and blue energy shifts are determined by emitter configuration and plasma parameters
- + spectra with different temperatures
- + the photon emission spectra are considered using different configurations to improve M^0 for the x-ray transitions in K_{α} L^N satellites

thank you

background: http://3.bp.blogspot.com/_P1mM2TTud6Y/SsNv3CM9mEI/AAAAAAAAABxY/INvsuM6tzsc/s1600-h/20090618-2039.jpg

Acknowledgments:

God, My parents, Heidi Reinholz, Gerd Röpke, Olga Rosmej, Jacek Rzdakiewicz, Andrea Sengebusch, Sonja Lorenzen, Thmoas Keil, Volker Mosert, Niels-Uwe Bastian, SFB652